DOI: 10.53469/jpce.2026.08(01).08

The Multi-Level Classification Strategy for Rock Surface 3D Point Clouds

Zhenmin Chen[1], Shengwu Qin[1,*], Yong Tao[2], Wendi Rao[2], Jiawei Qi[2], Jiayu Yan[1]

[1]State Key Laboratory of Deep Earth Exploration and Imaging, College of Construction Engineering, Jilin University, Changchun 130026, Jilin, China
[2]Jilin Geological Environment Monitoring Center (Jilin Geological Disaster Emergency Technical Guidance Center), Changchun 130021, Jilin, China
Correspondence Author, qinsw@jlu.edu.cn

Abstract: ***This study presents an integrated computational framework for accurate rock discontinuity characterization in complex geological environments, addressing the limitations of traditional field measurements and existing automated approaches through the synergistic combination of UAV-based remote sensing and advanced machine learning techniques. The methodology establishes a three-stage analytical pipeline beginning with an optimized Random Forest algorithm for robust initial classification of discontinuity features in 3D point cloud data, followed by Mean Shift clustering to systematically group discontinuities by principal orientations, and concluding with DBSCAN-based refinement for precise boundary delineation. Field validation demonstrates the framework's effectiveness in overcoming environmental noise and surface irregularity challenges, with the Mean Shift clustering component particularly excelling in maintaining geometric fidelity for complex curved or rough discontinuity surfaces. The approach shows consistent performance advantages over conventional methods in both detection accuracy and computational stability, offering practical improvements for geological surveys by enhancing measurement reliability while reducing field workload, with broad applications in slope stability assessment, underground excavation design, and rock mass quality evaluation.***

Keywords: Rock discontinuity analysis, UAV photogrammetry, Machine learning, Nonparametric clustering, 3D point cloud.

1. Introduction

Geological interfaces, or discontinuities, within rock masses result from various geological processes and are commonly found in rock formations (Wittke, 1990). These discontinuities preserve the mechanical properties of specific areas over long geological periods, encapsulating information about Earth's geological activities throughout its extensive history (Gong *et al*., 2021). Investigating the parameters of these discontinuities is essential for a comprehensive assessment and prediction of the stability, permeability, and mechanical properties of geological entities (Liang *et al*., 2023). A widely accepted approach is to develop discontinuity characterization models based on parameters derived from exposed rock surfaces, which can then be extended to the interior of rock masses (Gong *et al*., 2019, Jiang *et al*., 2020).

In practical applications, direct manual measurements of exposed discontinuities, conducted through physical contact, can yield reliable results (Priest, 1993). However, this approach is limited by safety concerns, inefficiency, and potential biases, making it impractical in inaccessible areas or regions with complex terrain, such as steep slopes (Kelam, 2022). The rapid development of remote sensing and computational technologies has facilitated the digitization of discontinuity measurements (Wasowski and Bovenga, 2022). Early studies primarily focused on acquiring discontinuity data by photographing exposed surfaces (Lane *et al*., 2000). Later research shifted towards using point cloud data for discontinuity identification, leveraging three-dimensional models of rock faces generated by remote sensing techniques like LiDAR and photogrammetry (Lato *et al*., 2009). Notably, image-based methods continue to be effective for capturing discontinuities orthogonal to rock surfaces (Azizi and Moomivand, 2021). In recent years, several studies have proposed various point cloud-based methods for identifying discontinuities (Gigli and Casagli, 2011). Undoubtedly, these methods have significantly advanced the digitization of discontinuity measurements. Nevertheless, due to the inherent complexity of natural environments, ongoing challenges in both data acquisition and discontinuity identification techniques remain, necessitating further resolution.

Data acquisition in complex environments poses significant challenges. Terrestrial laser scanning (TLS) is commonly employed by geoscientists and engineers for on-site data collection; however, its limited flexibility becomes particularly problematic in dense forests and rugged terrains (Singh *et al*., 2021a). To mitigate the impact of vegetation on scanner mobility, Singh *et al*. (2021) utilized handheld mobile laser scanning (H-MLS) for slope data acquisition. While H-MLS improves adaptability in complex settings, it still cannot reach areas beyond human access. Advances in optical sensors and manufacturing have resulted in lighter laser scanners. Mounting compact laser scanners on unmanned aerial vehicles (UAVs) enhances mobility and enables better adaptation to the constraints of complex terrain (Arslan Kelam *et al*., 2024). Compared to TLS and H-MLS, UAV-based mobile laser scanning offers distinct advantages in both flexibility and data acquisition efficiency.

The presence of various surface features significantly impacts the performance of discontinuity identification algorithms. Previous studies have employed coplanarity detection (Riquelme *et al*., 2015), region growing (Wang *et al*., 2017), filtering algorithms (Singh *et al*., 2021b), fast Fourier transforms (Singh *et al*., 2022), and other methods to extract discontinuity point sets from rock point clouds. These approaches exhibit effective noise resistance when processing simple, small-scale non-discontinuity data. However, when rock slopes are subjected to complex interferences—such as irregular discontinuities, multi-scale debris, slope shrubs, and

gravelly soil layers—point cloud processing often requires considerable manual effort (Menegoni *et al*., 2019). Fortunately, advances in computational power and the rapid development of machine learning technologies have introduced new tools for rock discontinuity identification. In recent years, researchers have begun exploring machine learning (ML) applications in this field (Yunfeng *et al*., 2022), utilizing artificial neural networks, gradient boosting trees, and similar methods for intelligent identification of discontinuities from 3D point clouds. Nevertheless, like earlier non-ML approaches, existing studies still fail to sufficiently account for the impact of complex environments on identification performance.

Determining the dominant orientations (main directions) of discontinuities presents significant challenges. Semi-automatic methods, which combine algorithmic support with manual expertise, are commonly used to identify the number of principal orientations. However, these methods heavily rely on the operator's expertise and experience (Riquelme *et al*., 2014). To achieve more objective identification of main directions, advanced algorithms, such as the cluster validity index (CVI) and clustering by fast search and find of density peaks (CFSFDP), have been applied to automatically determine the number of main directions (Chen *et al*., 2016). However, CVI requires multiple clustering iterations to evaluate the optimal number of clusters, leading to increased time costs. CFSFDP requires precomputing pairwise similarities between points, resulting in prohibitive computational and storage costs for large-scale data applications (Rodriguez and Laio, 2014). Therefore, there is a pressing need for an improved automated discontinuity extraction method to address the time and memory constraints associated with large point cloud datasets in practical applications.

Current discontinuity detection methods are often limited by the complexity of natural rock surfaces, affecting their practical applicability. This study proposes a hierarchical classification approach that combines machine learning with the mean shift clustering algorithm to accurately identify discontinuities under complex conditions. The method employs machine learning-based point cloud preprocessing to reduce environmental interference and utilizes the mean shift algorithm for orientation clustering. This flexible framework allows algorithm customization at different processing stages, significantly improving robustness for engineering applications while maintaining computational efficiency. The results demonstrate that this technique exhibits outstanding practical value for discontinuity identification in challenging field conditions.

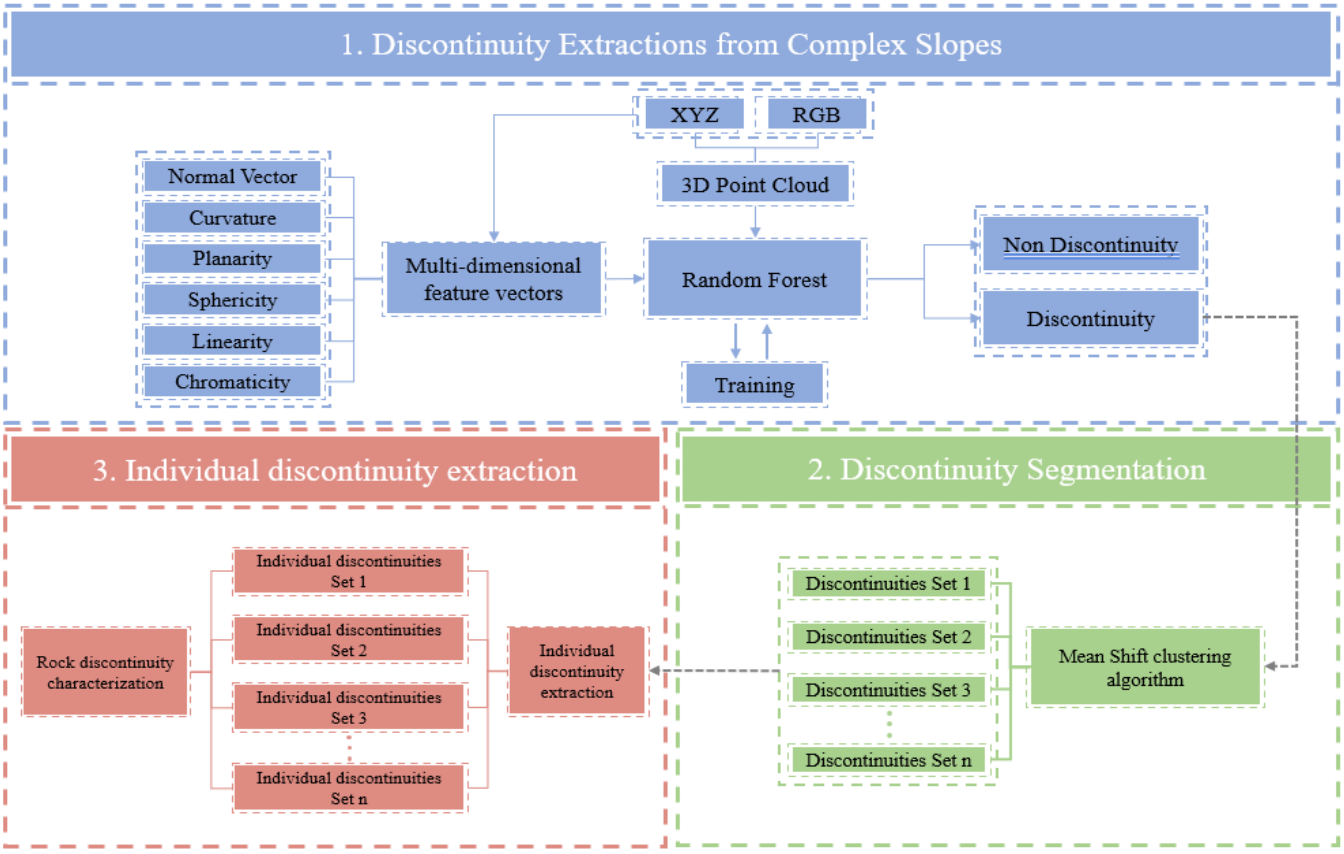

Figure 1: Flowchart of the proposed approach

2. Methodology

This study proposes a phased methodological framework (Figure 1) to address the multi-source interference affecting automatic identification of rock mass discontinuities in complex terrain environments. The developed methodology consists of five principal components:

Step1: The RGB images of the slope acquired via an unmanned aerial vehicle (UAV) platform were processed using the Structure from Motion (SfM) technique (Westoby *et al*., 2012). This photogrammetric approach reconstructs 3D models by extracting feature points from overlapping images captured at multiple viewing angles. Following point cloud

generation, a preliminary preprocessing step was implemented to establish a structured dataset containing spatial coordinates (X, Y, Z) and spectral attributes (R, G, B).

Step2: The k-d tree algorithm was integrated with KNN and PCA to compute local geometric features and normal vectors for each point cloud element. The output includes: a feature vector (C, P, S, V, R', G', B') representing local point characteristics, and normal vectors (N_x, N_y, N_z) calculated from each point's spatial relationship with its neighbors.

Step3: A Bayesian optimization-based parameter space search strategy was implemented on the point feature dataset generated in Step 2 to systematically determine the optimal hyperparameter configuration for the Random Forest (RF) classifier. Subsequently, a high-performance RF model was trained using the complete sample set with optimized parameters, achieving holistic classification of the point cloud data. Throughout this process, geometric coordinates (X, Y, Z) and localized normal vectors (N_x, N_y, N_z) were synchronously extracted for spatial points identified as discontinuity surfaces.

Step4: All normal vectors of the discontinuity points acquired in Step 3 were assigned to their corresponding primary discontinuity sets using the mean shift clustering algorithm based on orientation similarity. Subsequently, the Density-Based Spatial Clustering of Applications with Noise (DBSCAN) algorithm was applied to analyze spatial coordinates within each discontinuity set, enabling the isolation of individual discontinuity planes.

Step5: The Random Sample Consensus (RANSAC) algorithm was employed to perform planar fitting on each clustered subset obtained from the preceding step, followed by quantitative determination of the dip direction and dip angle parameters of structural discontinuities through three-dimensional geometric analysis.

2.1 Feature Extraction

2.1.1 Normal vectors

The point normal vector, a critical local geometric descriptor of 3D point clouds, is defined as the unit orthogonal vector to the least-squares fitted local plane. To address large-scale point cloud processing, the algorithm employs k-d tree spatial partitioning to optimize KNN search efficiency. Principal Component Analysis on the neighborhood points constructs a 3D covariance matrix, whose eigenvalues $\lambda_1 \geq \lambda_2 \geq \lambda_3 \geq 0$ and orthonormal eigenvectors $\{v_1, v_2, v_3\}$ are computed. The unit normal vector $n = (n_x, n_y, n_z)$ is derived from eigenvector v_3 corresponding to the minimal eigenvalue λ_3, with directional consistency enforced through global orientation constraints.

2.1.2 Point Features

In 3D point cloud datasets, the local geometric features of discrete points characterize the spatial relationships with their neighboring points. These features essentially constitute a multidimensional attribute collection of the point cloud, enabling attribute-difference-based point cloud classification through the provision of distinguishable feature descriptors for machine learning models.

Geometric Features: In point cloud classification tasks, geometric features serve as critical classification criteria that characterize the morphological attributes of local point clusters. Building upon the seminal work of (Weinmann *et al*., 2013) on geometric feature redundancy analysis, this study adopts curvature (C), planarity (P), and sphericity (S) as discriminative geometric descriptors. The mathematical formulations of these parameters are expressed as follows:

$$C = \frac{\lambda_3}{\lambda_1+\lambda_2+\lambda_3} \quad (1)$$

$$P = \frac{\lambda_2-\lambda_3}{\lambda_1} \quad (2)$$

$$S = \frac{\lambda_3}{\lambda_1} \quad (3)$$

where λ_1, λ_2, and λ_3 are the eigenvalues of the covariance matrix of the coordinate set of the query point and its neighboring points, with $\lambda_1 \geq \lambda_2 \geq \lambda_3 \geq 0$.

Slope: Based on the feature quantification framework established by Weinmann *et al*. (Weinmann *et al*., 2013), this study designates verticality (V) as a pivotal descriptor for characterizing slope morphology, which holds second-tier significance in feature contribution evaluation. Recent research by Beni *et al*. (Beni *et al*., 2023) has systematically substantiated the discriminative efficacy of this feature metric through multi-source point cloud data integration, particularly evident in its sensitivity to structural plane classification within complex terrain conditions. The mathematical formulation is expressed as:

$$V = 1 - n_z \quad (4)$$

where n_z denotes the third component of the point normal vector n.

Color: Within 3D point cloud classification methodological frameworks, spectral attributes have been established as critical discriminative parameters. Chroma is a simple feature that remains constant regardless of variations in the emitted light intensities (Cernadas *et al*., 2017). The specific calculation is formulated as follows:

$$R' = \frac{\mathrm{R}}{\mathrm{R}+G+B} \quad (5)$$

$$G' = \frac{\mathrm{G}}{\mathrm{R}+G+B} \quad (6)$$

$$B' = \frac{\mathrm{B}}{\mathrm{R}+G+B} \quad (7)$$

where *R*, *G*, and *B* denote the chromaticity values of the red, green, and blue channels, respectively.

2.2 Rock Discontinuity Intelligent Extraction

2.2.1 Random Forest

Random Forest (RF), a machine learning algorithm constructed by integrating multiple decorrelated decision trees, demonstrates robust resistance to overfitting in handling high-dimensional classification tasks (Breiman, 1996). This study employs the RF algorithm for multi-target classification of rock slope point clouds. By fusing normal vector verticality, chromaticity space and local curvature distribution, the

method achieves effective identification of rock mass discontinuities. The target categories—vegetation, structural discontinuities, and unconsolidated deposits—are defined based on spectral reflectance discrepancies and three-dimensional spatial topological relationships within the point cloud data. During node splitting, the algorithm randomly selects feature subsets and determines optimal splitting thresholds through the Gini index minimization criterion. The Gini index is calculated as:

$$Gini(D) = 1 - \sum_{k=1}^{K} \left(\frac{|C_k|}{|D|}\right)^2 \quad (4)$$

let D denote the dataset, where C_k represents the subset of samples belonging to the k-th class, and K indicates the total number of classes. The Gini index quantifies node impurity, with lower values corresponding to higher node purity. The feature achieving maximal purity gain through binary splitting is identified as the optimal splitting feature.

2.2.2 Bayesian Optimization

Bayesian optimization algorithms are widely employed for hyperparameter optimization tasks due to their capability to rapidly identify optimal configurations (Sameen *et al*., 2020, Sun *et al*., 2021). When analytical expressions of objective functions are unavailable or computationally intractable, these algorithms construct Gaussian process (GP) surrogate models to estimate the behavior of the objective function (Bull, 2011, Gelbart *et al*., 2014). The critical hyperparameters governing random forest (RF) performance comprise: NumTrees (number of decision trees), MaxNumSplits (maximum splitting operations per tree), and NumPredictorstoSample (feature candidates per node split). In this study, these three hyperparameters are designated as input variables, with fivefold cross-validation accuracy serving as the output response. The Bayesian optimization framework is employed to determine the optimal hyperparameter configuration for the RF model.

2.2.3 Model Evaluation

To validate the efficacy of the optimized model, we employ confusion matrix-derived metrics (accuracy, precision, and recall) to quantitatively assess classification performance. These metrics are formally defined as:

$$Accuracy = \frac{TP+TN}{TP+TN+FP+FN} \quad (9)$$

$$Precision = \frac{TP}{TP+FP} \quad (10)$$

$$Recall = \frac{TP}{TP+FN} \quad (11)$$

where TP (True Positive) denotes correctly classified positive instances, FN (False Negative) represents misclassified positive instances, FP (False Positive) indicates misclassified negative instances, and TN (True Negative) refers to correctly classified negative instances. The qualifier "True" signifies correct classification, "Positive" corresponds to the target class, "False" indicates misclassification, and "Negative" refers to non-target classes.

2.3 Discontinuity Segmentation in Point Clouds

2.3.1 Discontinuity Set Identification

The identification of discontinuity sets constitutes a fundamental procedure for the refined characterization of rock mass structural planes. The core objective lies in achieving accurate partitioning of discrete point clouds into corresponding discontinuity sets based on their spatial distribution characteristics. This study employs the Mean Shift clustering algorithm based on density gradient estimation, which performs cluster analysis through iterative search for local density maxima within point cloud data. By defining a dynamic window via kernel functions, the algorithm progressively updates centroid positions along the probability density gradient direction until convergence to stable cluster centers. Compared with conventional clustering methods, the proposed algorithm exhibits the following distinctive advantages: (1) It eliminates the need for predefining cluster quantities and adaptively identifies structural plane point sets with arbitrary spatial topologies; (2) Only the bandwidth parameter is required to control clustering precision, while demonstrating robust anti-interference capability against measurement noise and outliers.

2.3.2 Recognition of individual discontinuity

To accurately calculate individual discontinuity set parameters, a secondary clustering process is implemented to subdivide each discontinuity from the principal orientation cluster. The DBSCAN (Density-Based Spatial Clustering of Applications with Noise) algorithm is employed for this hierarchical classification, enabling the identification of distinct planar features with similar spatial distributions within the primary cluster. As a robust density-based clustering algorithm, DBSCAN initiates by randomly selecting an XYZ coordinate (designated as point p) from the principal cluster. A predefined radial distance (eps) establishes a neighborhood around the selected seed point. When the number of neighboring points within this radius meets or exceeds a specified minimum threshold (MinPts), point p is classified as a core point. Conversely, points failing to satisfy this density criterion are categorized as border points. All core points and their associated neighboring points within the eps radius are subsequently grouped into a cohesive cluster. This iterative process continues until all density-reachable core points are assigned to corresponding clusters, while isolated core points form new cluster entities.

2.4 Plane Fitting

The RANSAC method is an iterative algorithm that can estimate the parameters of a fitted surface model from a dataset (Raguram *et al*., 2008, FISCHLER AND, 1981). It is extensively used for shape detection (Nguyen and Le, 2013, Xu *et al*., 2015), including the identification of building façades (Adam *et al*., 2018, Boulaassal *et al*., 2007) and roof (Chen *et al*., 2014). The computational workflow initiates by randomly selecting three non-collinear points to establish parametric plane models through linear equation derivation, followed by iterative verification of geometric consistency among neighboring points against predefined spatial tolerance thresholds. Points satisfying this proximity criterion are aggregated into an inlier consensus set, while those exceeding the threshold are classified as statistical outliers. Through cyclic hypothesis generation and validation, the planar configuration exhibiting maximum consensus set cardinality

is retained as the optimal solution. Subsequent removal of inlier-associated data points triggers search domain reinitialization, with this iterative process persisting until exhaustive detection of latent planar surfaces is achieved. Final surface validation is governed by consensus set population metrics, systematically discarding plane hypotheses demonstrating subcritical inlier densities while preserving geometrically significant surfaces with substantial consensus point concentrations.

RANSAC implementation yields the plane equation in the form of (Ax + By + Cz + D = 0), where A, B, and C are the unit normal vector components of the best-fit plane. The dip and the dip direction of the planes are found using Eqs. (12) and (13).

$$Dip\ direction = \begin{cases} 90 - \tan^{-1}\left(\frac{B}{A}\right) & A > 0 \\ 0° & A = 0\ and\ B \geq 0 \\ 180° & A = 0\ and\ B < 0 \\ 270 - \tan^{-1}\left(\frac{B}{A}\right) & A < 0 \end{cases} \quad (12)$$

$$Dip = \begin{cases} 0° & A^2 + B^2 = 0 \\ 90 - \tan^{-1}\left(\frac{|C|}{\sqrt{A^2+B^2}}\right) & A^2 + B^2 \neq 0 \end{cases} \quad (13)$$

3. Results

This study utilized a DJI Mavic 3E unmanned aerial vehicle (UAV) equipped with an integrated Real-Time Kinematic (RTK) positioning system for photogrammetric data acquisition. To preserve detailed slope characteristics, an oblique flight path was employed during data collection, maintaining a constant distance of 10 meters between the UAV and the target rock slope surface. An image overlap rate of 80% was configured to ensure sufficient tie points for subsequent 3D model reconstruction. A representative rock slope along a highway in Yanbian Korean Autonomous Prefecture, Jilin Province, China was selected as the case study (Figure 2), featuring an inclination angle of approximately 60° with sandstone as the predominant lithology.

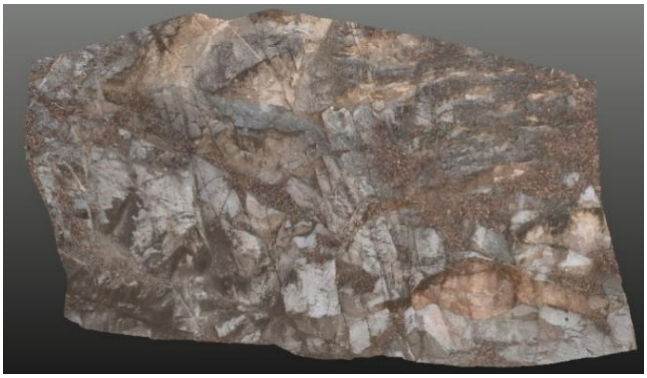

Figure 2: Point clouds of the research case

The field data presented in Figure 3 were classified into two distinct categories: a discontinuity dataset comprising 113,264 points (marked in yellow) and a non-discontinuity dataset containing 135,629 points (marked in blue). To determine the optimal neighborhood size (k) for feature extraction, we conducted an analysis of the discontinuity dataset, where the normal vectors of fracture planes were expected to converge with increasing sampling scale.

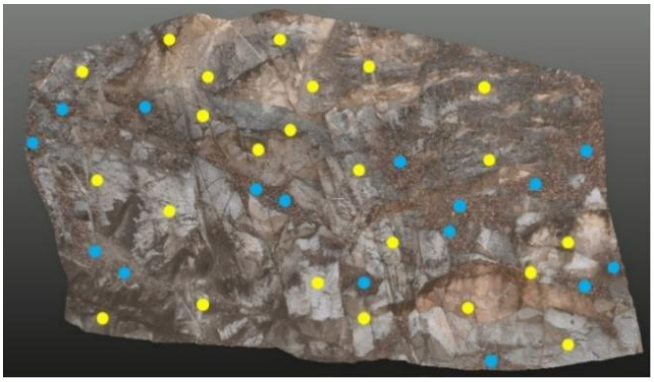

Figure 3: Learning samples. The yellow point clouds are the rock discontinuity sampling points, and the biue point clouds are the non-discontinuity sampling points

Prior to model training, we implemented class-balanced sampling by randomly selecting 100,000 data points from each category, resulting in a balanced dataset comprising 200,000 points in total. The dataset was then partitioned into training and validation subsets with an 8:2 ratio, where the training set served for model development and parameter optimization while the validation set was reserved for performance evaluation. For hyperparameter tuning, we employed Bayesian optimization coupled with five-fold cross-validation, executing 50 optimization iterations with classification accuracy as the evaluation metric. The optimal parameter configuration identified through this systematic process is presented in Table 1.

Table 1: RF hyperparameters obtained via Bayesian optimization

Hyperparameter	Searching space	Value
Number of learners	[10–500]	375
Maximum number of splits	[1–319999]	454891
Number of predictors to sample	[1–9]	5

To maximize feature learning from the complete dataset, we trained the final model using optimized hyperparameters, successfully classifying all slope point clouds and labeling a total of 3,291,750 discontinuity points. As illustrated in Figure 5, the classified discontinuity points are superimposed on the original point cloud for visual verification. While the classifier missed some high-roughness discontinuity points, the overall identification accuracy remains satisfactory. During the identification process, large rough discontinuities may appear as fragmented patches while maintaining structural integrity, whereas smaller rough discontinuities might be filtered out as scattered points - a reasonable compromise given that even expert geologists often struggle to distinguish such features from debris. For the classified discontinuity point cloud, the Mean Shift (MS) algorithm automatically identified six principal discontinuity sets, completing the secondary classification. All discontinuity points were then grouped according to their principal orientations. The clustering results are visually presented in Figure 6 by overlaying directional subsets with the original point cloud. Finally, DBSCAN segmentation was applied to each principal orientation set, extracting 313 individual discontinuities and completing the tertiary classification. This comprehensive approach ensures complete discontinuity extraction while maintaining computational efficiency.

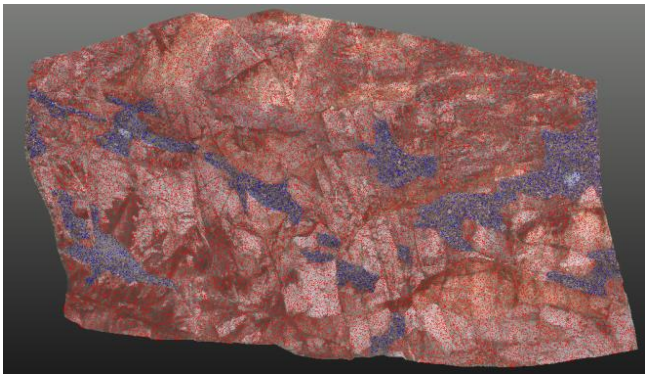

Figure 5: The results of identification and classification of all discontinuities and non-discontinuities

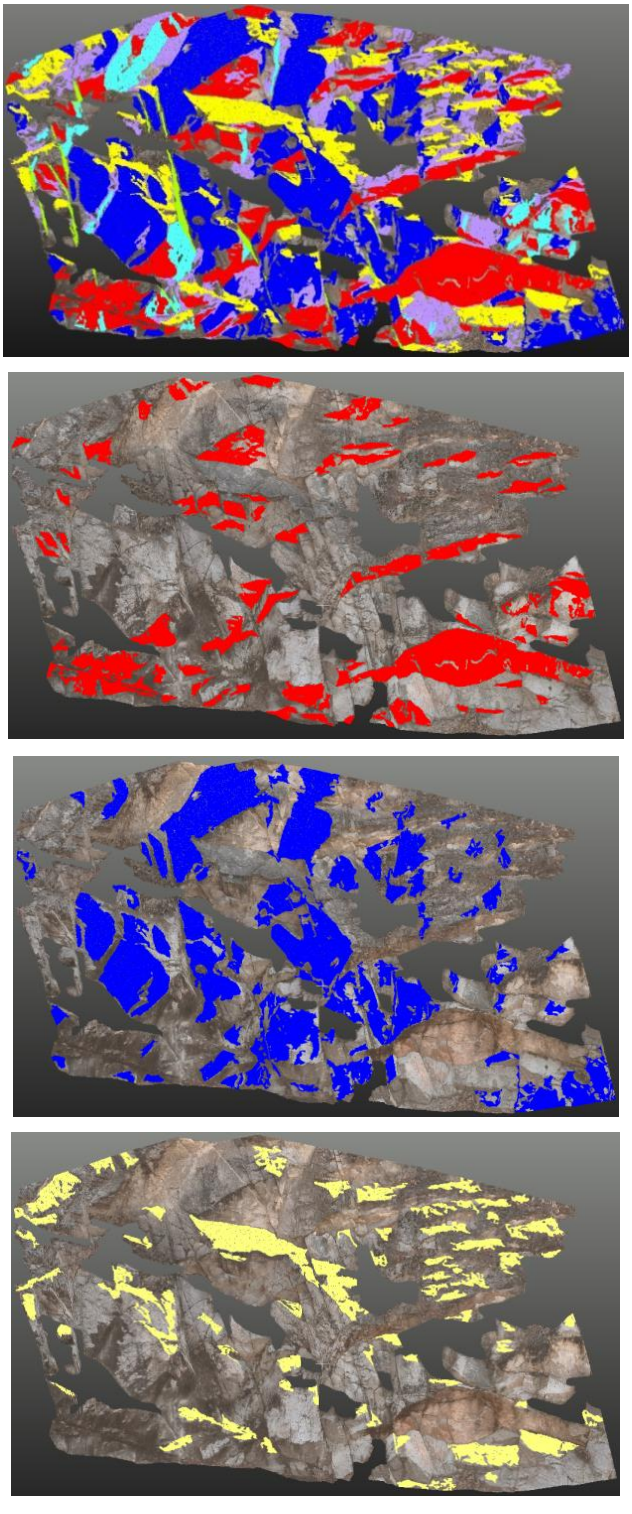

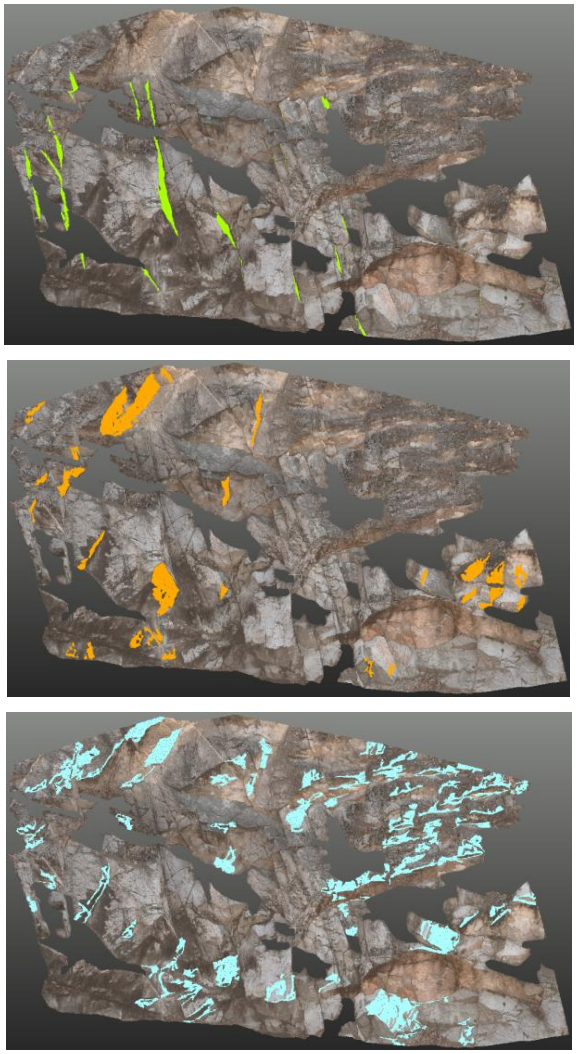

Figure 6: Discontinuity identification and classification result. The point clouds shown in each specific color represent the rock discontinuities identified as belonging to the same set.

4. Discussion

The deployment of unmanned aerial vehicles (UAVs) has revolutionized rock slope investigations in challenging environments. Compared to terrestrial laser scanning (TLS) and handheld mobile laser scanning (H-MLS) systems, UAV-mounted platforms offer unparalleled flexibility to navigate along slope profiles, significantly minimizing scan occlusions while capturing high-fidelity point cloud data. Although this aerial approach effectively overcomes environmental constraints during data acquisition, the critical challenge of accurately identifying and differentiating discontinuities from other geological features within complex rock mass formations remains unresolved. While the technology primarily addresses data collection limitations, it does not fundamentally solve the core problem of automated discontinuity recognition in heterogeneous slope conditions.

To effectively identify discontinuities in complex geological environments, this study proposes a multi-stage hierarchical processing framework. The methodology is systematically organized into three progressive phases: initial point cloud classification, followed by orientation-based clustering, and concluding with individual discontinuity extraction. This structured approach integrates the strengths of supervised

learning for complex feature recognition with the efficiency of unsupervised techniques for segmentation tasks, ensuring both comprehensive coverage and high-precision results.

4.1 Performance of the RF Classifier

To evaluate the effectiveness of the model, the optimized version with tuned hyperparameters was applied to classify the test dataset. Performance was assessed using confusion matrix analysis, which yielded an overall classification accuracy of 89.2% for discontinuity identification (Figure 7). This result significantly surpasses the minimum practical threshold of 60–70% accuracy proposed by Weidner and Walton for engineering geology applications, a benchmark derived from their comprehensive analysis of 2,560 random forest classifiers. The achieved performance underscores the model's reliability and confirms its suitability for practical use in rock discontinuity analysis.

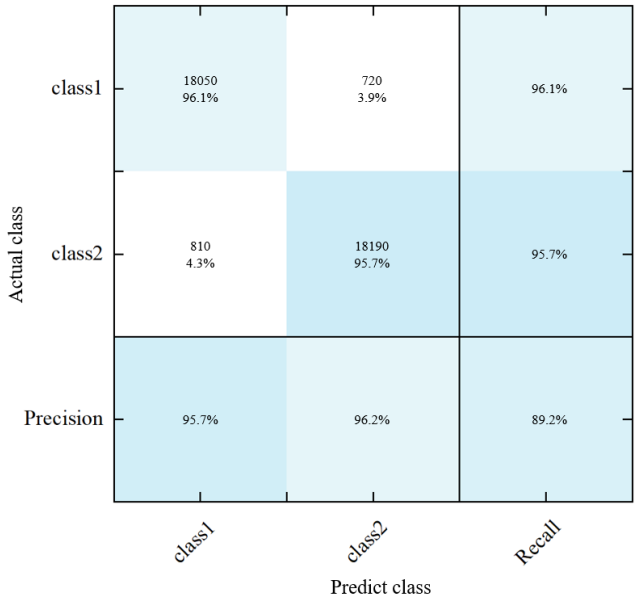

Figure 7: The confusion matrix of test set.

The discontinuity category demonstrates superior performance, with precision and recall reaching 95.7% and 96.1%, respectively. The feature selection strategy prioritizes planar structural characteristics, such as geometric attributes and local descriptors, which enhances the ability of the random forest model to effectively identify discontinuities. This approach not only improves detection accuracy but also maintains interpretability for non-specialists. In practice, the study adopts a balanced approach by incorporating fundamental features like color and slope, thereby avoiding unnecessary complexity that could arise from over-optimizing the classification of secondary geographic elements. The established performance threshold considers discontinuities satisfactory when both precision and recall exceed 90%, a standard well above the minimum acceptable level for geological applications.

The classification performance varies among non-discontinuity categories. This inter-class confusion phenomenon corroborates findings reported by Weidner and Walton, indicating inherent limitations in distinguishing between soil and fractured regions using conventional point cloud features. While advanced analytical methods could potentially enhance discrimination, such refinements fall beyond the scope of this study, which primarily focuses on discontinuity identification. From a practical engineering perspective, the current classification performance for all non-discontinuity categories remains operationally viable, given that the primary objective is accurate discontinuity detection rather than exhaustive classification of non-discontinuity features.

The developed classifier may however demonstrate constrained generalizability—a prevalent issue in geoscience applications owing to substantial geographical variations in natural features. While enhancing model generalizability frequently involves trade-offs with recognition accuracy, our methodology emphasizes high-precision identification tailored for localized engineering applications. Given the rigorous accuracy requirements for discontinuity measurements and the inherently site-specific nature of construction projects, we intentionally trained the machine learning model exclusively on data from the study area. This localized training approach aligns with prevailing best practices in engineering applications, where models are customarily developed for specific regional contexts rather than universal applicability.

4.2 The Effectiveness of the Main Direction Identification

Through visual comparative analysis, the identification results of rock discontinuity sets in each case demonstrated a high degree of consistency with the manually measured data. When identifying rock surfaces with well-developed planar features, the recognition results exhibited large-scale continuous clusters of point clouds belonging to a single category. Taking the J1 discontinuity set in the case as an example, which represents a near-slope aspect structural plane with wide distribution and good extensibility, the identification results accurately reflected the spatial distribution characteristics of this discontinuity set. For complex rock mass areas where local planar features change significantly or multiple structural planes intersect, the identification results showed that the point clouds corresponding to different discontinuity sets exhibited a mutually intersecting and overlapping distribution pattern. During the research process, the system did not forcibly merge point clouds from different discontinuity sets in localized regions. Instead, distinctions were made based on their actual characteristics, effectively preserving the local geometric morphology and spatial distribution details of different rock structural planes. Furthermore, for discontinuity sets with low distribution density and limited spatial extent, such as the J3 set, the method also achieved accurate identification and reasonable classification, demonstrating the algorithm's capability to handle sparse data.

In the comparative analysis of orientation measurement results, the largest discrepancy occurred in the J3 discontinuity set, with a maximum dip angle error of 3.74°. This discrepancy primarily stems from the inherent complexity of the field data: the discontinuities of the J3 set are spatially dispersed, and the number of data points is relatively low, resulting in less pronounced statistical characteristics of the orientation compared to other sets. This data sparsity and distribution discreteness increase the difficulty of accurate identification and orientation

measurement, which constitutes the main cause of the error. Nonetheless, the error remains within the acceptable range for engineering geological applications, and algorithmic optimizations have further reduced the impact of such errors.

5. Conclusion

This study presents an innovative methodology system for intelligent identification and characterization of rock discontinuities, which integrates unmanned aerial vehicle (UAV) photogrammetry with machine learning technologies. The method employs a multi-level classification strategy, combining random forest classification, mean shift clustering, and DBSCAN segmentation algorithms to construct a comprehensive automated analysis framework. Initially, high-resolution 3D point cloud data is acquired via UAV, and an optimized random forest classifier is utilized to accurately identify structural planes. Subsequently, mean shift clustering is applied to intelligently group the orientation characteristics of the structural planes, followed by the use of the DBSCAN algorithm to extract individual discontinuities. The entire workflow adopts a hierarchical and progressive approach, integrating multi-dimensional features—including geometric, spectral, and spatial data—which effectively mitigates common engineering interferences such as complex terrain, vegetation coverage, and irregular structural planes, thereby significantly improving analytical accuracy.

The method demonstrates excellent engineering applicability. Its flexible framework supports parameter adjustment and functional expansion, while the use of a UAV platform overcomes the spatial limitations inherent in traditional surveying equipment. Compared with conventional methods such as terrestrial laser scanning, this technique offers distinct advantages in terms of operational efficiency, data coverage, and safety—making it particularly suitable for hazardous environments such as high and steep slopes. The technology enables a fully automated workflow from data acquisition to analysis, not only enhancing the efficiency and accuracy of structural plane investigations, but also providing reliable technical support for the evaluation of rock mass stability and the prevention of geological hazards. It holds strong potential to become a vital technical tool in the field of geological surveying.

References

[1] ADAM, A., CHATZILARI, E., NIKOLOPOULOS, S. & KOMPATSIARIS, I. (2018), "H-RANSAC: A hybrid point cloud segmentation combining 2D and 3D data", *ISPRS Annals of the Photogrammetry, Remote Sensing and Spatial Information Sciences*, Vol. 41-8.

[2] ARSLAN KELAM, A., AKGÜN, H., BOBET, A. & KOÇKAR, M. K. (2024), "Engineering geological characterization and assessment of complex rock slope failures in Mudurnu, Turkey", *Natural Hazards*, Vol. 120 No. 4, pp. 3271-3298.

[3] AZIZI, A. & MOOMIVAND, H. (2021), "A new approach to represent impact of discontinuity spacing and rock mass description on the median fragment size of blasted rocks using image analysis of rock mass", *Rock Mechanics and Rock Engineering*, Vol. 54 No. 4, pp. 2013-2038.

[4] BENI, T., NAVA, L., GIGLI, G., FRODELLA, W., CATANI, F., CASAGLI, N., GALLEGO, J. I., MARGOTTINI, C. & SPIZZICHINO, D. (2023), "Classification of rock slope cavernous weathering on UAV photogrammetric point clouds: The example of Hegra (UNESCO World Heritage Site, Kingdom of Saudi Arabia)", *Engineering Geology*, Vol. 325107286.

[5] BOULAASSAL, H., LANDES, T., GRUSSENMEYER, P. & TARSHA-KURDI, F. (2007), "Automatic segmentation of building facades using terrestrial laser data", in *ISPRS Workshop on Laser Scanning 2007 and SilviLaser 2007*, pp. 65-70.

[6] BREIMAN, L. (1996), "Bagging predictors", *Machine learning*, Vol. 24123-140.

[7] BULL, A. D. (2011), "Convergence rates of efficient global optimization algorithms.", *Journal of Machine Learning Research*, Vol. 12 No. 10, pp.

[8] CERNADAS, E., FERNANDEZ-DELGADO, M., GONZÁLEZ-RUFINO, E. & CARRIÓN, P. (2017), "Influence of normalization and color space to color texture classification", *Pattern Recognition*, Vol. 61120-138.

[9] CHEN, D., ZHANG, L., MATHIOPOULOS, P. T. & HUANG, X. (2014), "A methodology for automated segmentation and reconstruction of urban 3-D buildings from ALS point clouds", *IEEE Journal of Selected Topics in Applied Earth Observations and Remote Sensing*, Vol. 7 No. 10, pp. 4199-4217.

[10] CHEN, J., ZHU, H. & LI, X. (2016), "Automatic extraction of discontinuity orientation from rock mass surface 3D point cloud", *Computers & geosciences*, Vol. 9518-31.

[11] FISCHLER AND, M. A. (1981), "Random sample consensus: a paradigm for model fitting with applications to image analysis and automated cartography", *Commun. ACM*, Vol. 24 No. 6, pp. 381-395.

[12] GELBART, M. A., SNOEK, J. & ADAMS, R. P. (2014), "Bayesian optimization with unknown constraints", *arXiv preprint arXiv:1403.5607*,.

[13] GIGLI, G. & CASAGLI, N. (2011), "Semi-automatic extraction of rock mass structural data from high resolution LIDAR point clouds", *International journal of rock mechanics and mining sciences*, Vol. 48 No. 2, pp. 187-198.

[14] GONG, W., JUANG, C. H. & WASOWSKI, J. (2021), "Geohazards and human settlements: Lessons learned from multiple relocation events in Badong, China–Engineering geologist's perspective", *Engineering Geology*, Vol. 285106051.

[15] GONG, W., TANG, H., WANG, H., WANG, X. & JUANG, C. H. (2019), "Probabilistic analysis and design of stabilizing piles in slope considering stratigraphic uncertainty", *Engineering Geology*, Vol. 259105162.

[16] JIANG, Z., MALLANTS, D., GAO, L., MARIETHOZ, G. & PEETERS, L. (2020), "Surf3DNet1. 0: A deep learning model for regional-scale 3D subsurface structure mapping", *Geoscientific Model Development Discussions*, Vol. 20201-11.

[17] KELAM, A. A. (2022) Engineering geological characterization of the rock masses and their evaluation by spatial analyses, determination of the rock slope failure susceptibility zones and hazard assessment of

Mudurnu (Bolu)., Middle East Technical University (Turkey).
[18] LANE, S. N., JAMES, T. D. & CROWELL, M. D. (2000), "Application of digital photogrammetry to complex topography for geomorphological research", *The Photogrammetric Record*, Vol. 16 No. 95, pp. 793-821.
[19] LATO, M., DIEDERICHS, M. S., HUTCHINSON, D. J. & HARRAP, R. (2009), "Optimization of LiDAR scanning and processing for automated structural evaluation of discontinuities in rockmasses", *International Journal of Rock Mechanics and Mining Sciences*, Vol. 46 No. 1, pp. 194-199.
[20] LIANG, X., XU, T., CHEN, J. & JIANG, Z. (2023), "A deep-learning based model for fracture network characterization constrained by induced micro-seismicity and tracer test data in enhanced geothermal system", *Renewable Energy*, Vol. 216119046.
[21] MENEGONI, N., GIORDAN, D., PEROTTI, C. & TANNANT, D. D. (2019), "Detection and geometric characterization of rock mass discontinuities using a 3D high-resolution digital outcrop model generated from RPAS imagery–Ormea rock slope, Italy", *Engineering geology*, Vol. 252145-163.
[22] NGUYEN, A. & LE, B. (2013), "3D point cloud segmentation: A survey", in *2013 6th IEEE conference on robotics, automation and mechatronics (RAM)*, IEEE, pp. 225-230.
[23] PRIEST, S. D. (1993), Discontinuity analysis for rock engineering, Springer Science & Business Media.
[24] RAGURAM, R., FRAHM, J. & POLLEFEYS, M. (2008), "A comparative analysis of RANSAC techniques leading to adaptive real-time random sample consensus", in *Computer Vision–ECCV 2008: 10th European Conference on Computer Vision, Marseille, France, October 12-18, 2008, Proceedings, Part II 10*, Springer, pp. 500-513.
[25] RIQUELME, A. J., ABELLÁN, A. & TOMÁS, R. (2015), "Discontinuity spacing analysis in rock masses using 3D point clouds", *Engineering geology*, Vol. 195185-195.
[26] RIQUELME, A. J., ABELLÁN, A., TOMÁS, R. & JABOYEDOFF, M. (2014), "A new approach for semi-automatic rock mass joints recognition from 3D point clouds", *Computers & geosciences*, Vol. 6838-52.
[27] RODRIGUEZ, A. & LAIO, A. (2014), "Clustering by fast search and find of density peaks", *science*, Vol. 344 No. 6191, pp. 1492-1496.
[28] SAMEEN, M. I., PRADHAN, B. & LEE, S. (2020), "Application of convolutional neural networks featuring Bayesian optimization for landslide susceptibility assessment", *Catena*, Vol. 186104249.
[29] SINGH, S. K., BANERJEE, B. P., LATO, M. J., SAMMUT, C. & RAVAL, S. (2022), "Automated rock mass discontinuity set characterisation using amplitude and phase decomposition of point cloud data", *International Journal of Rock Mechanics and Mining Sciences*, Vol. 152105072.
[30] SINGH, S. K., RAVAL, S. & BANERJEE, B. P. (2021a), "Automated structural discontinuity mapping in a rock face occluded by vegetation using mobile laser scanning", *Engineering Geology*, Vol. 285106040.
[31] SINGH, S. K., RAVAL, S. & BANERJEE, B. P. (2021b), "Automated structural discontinuity mapping in a rock face occluded by vegetation using mobile laser scanning", *Engineering Geology*, Vol. 285106040.
[32] SUN, D., XU, J., WEN, H. & WANG, D. (2021), "Assessment of landslide susceptibility mapping based on Bayesian hyperparameter optimization: A comparison between logistic regression and random forest", *Engineering Geology*, Vol. 281105972.
[33] WANG, X., ZOU, L., SHEN, X., REN, Y. & QIN, Y. (2017), "A region-growing approach for automatic outcrop fracture extraction from a three-dimensional point cloud", *Computers & geosciences*, Vol. 99100-106.
[34] WASOWSKI, J. & BOVENGA, F. (2022), "Remote sensing of landslide motion with emphasis on satellite multi-temporal interferometry applications: An overview", *Landslide hazards, risks, and disasters*, 365-438.
[35] WEINMANN, M., JUTZI, B. & MALLET, C. (2013), "Feature relevance assessment for the semantic interpretation of 3D point cloud data", *ISPRS Annals of the Photogrammetry, Remote Sensing and Spatial Information Sciences*, Vol. 2313-318.
[36] WESTOBY, M. J., BRASINGTON, J., GLASSER, N. F., HAMBREY, M. J. & REYNOLDS, J. M. (2012), "'Structure-from-Motion' photogrammetry: A low-cost, effective tool for geoscience applications", *Geomorphology*, Vol. 179300-314.
[37] WITTKE, W. (1990), Rock mechanics, Springer-Verlag Berlin.
[38] XU, B., JIANG, W., SHAN, J., ZHANG, J. & LI, L. (2015), "Investigation on the weighted ransac approaches for building roof plane segmentation from lidar point clouds", *Remote Sensing*, Vol. 8 No. 1, pp. 5.
[39] YUNFENG, G., BEI, C. & TANG, H. (2022), "Rock Discontinuities Identification from 3D Point Clouds Using Artificial Neural Network", *Rock Mechanics and Rock Engineering*, Vol. 55 No. 3, pp. 1705-1720.